Original article

Isobavachalcone induces apoptosis of colorectal cancer cells mediated by interaction with survivin: Experimental and theoretical analyses

Li Zhang [a,1], Bo Yi [b,1], Jing Chen [a,*]

[a] Department of Medical Oncology, Sichuan Clinical Research Center for Cancer, Sichuan Cancer Hospital & Institute, Sichuan Cancer Center, Affiliated Cancer Hospital of University of Electronic Science and Technology of China, Chengdu 610041, China
[b] Department of Colorectal Surgery, Sichuan Clinical Research Center for Cancer, Sichuan Cancer Hospital & Institute, Sichuan Cancer Center, Affiliated Cancer Hospital of University of Electronic Science and Technology of China, Chengdu 610041, China

ARTICLE INFO

ABSTRACT

Isobavachalcone (IBC) as a bioactive chalcone isolated from the seeds of *Psoralea corylifolia* Linn has shown promising anticancer activities. However, its main anticancer mechanism in colorectal cancer cells has not been well-explored. Recently, the interaction of therapeutic compounds with survivin, an antiapoptotic marker, has been indicated to be a potential approach for advancing anticancer compounds. Therefore, in this study, IBC was evaluated for its anticancer activities against metastatic colorectal adenocarcinoma, LoVo, followed by exploring its interaction with survivin. It was observed that incubation of the human LoVo colorectal cancer cells with the IBC at 24 h resulted in a significant reduction in cell viability with an IC_{50} of about 35 μM as well as a significant membrane damage. Also, it was deduced that IBC could result in the formation of excessive ROS, lipid peroxidation, reduction of SOD/CAT activity, as well as downregulation of Nrf2 and HO-1 mRNA levels. Further studies showed that IBC could induce MMP reduction, cytochrome c (Cyt c) release, overexpression of Bax/Bcl-2 mRNA ratio as well as caspase-9 and −3. Moreover, it was deduced that IBC mitigated the expression of survivin at mRNA and protein levels. Then, binding parameters indicated that IBC strongly binds to one molecule of survivin at physiological temperature. Also, it was revealed that IBC substantially induced the conformational changes of survivin. Ultimately, through hydrogen bonding and hydrophobic forces, IBC has a substantial binding affinity with survivin (–9.80 kcal/mol) at a region that is critical to the dimerization process, according to molecular docking studies. Overall, this study showed that IBC may be used in future research to assess its clinical and *in vivo* behaviors in the modulation of colorectal cancer mediated by deactivation and downregulation of antiapoptotic survivin.

1. Introduction

Psoralea corylifolia L. referred to as "Bu-gu-zhi" in Chinese has been widely recruited as a crucial herb in traditional Chinese medicine (TCM) (Chen et al., 2023; Jiangning et al., 2005). Isobavachalcone (IBC, Scheme 1) as a prenylated chalcone was firstly extracted from the seeds of Bu-gu-zhi by Bhalla, Nayak et al. (Bhalla et al., 1968).

IBC has shown a wide range of activities such as anti-microbial, antioxidant, anti-inflammatory, anti-cancer, and neuroprotective effects (Wang et al., 2021). For example, it has been shown that IBC has potential anticancer activities against leukemia through induction a non-apoptotic/apoptotic cell death, reduction of mitochondrial membrane potential (MMP), and inhibition of dihydroorotate dehydrogenase (Yang et al., 2019; Li-li et al., 2014; Wu et al., 2018). Moreover, IBC has shown promising antiproliferative activity against prostate cancer cells (PC-3, LNCaP) mediated by induction of oxidative stress, apoptosis, inhibition of TrxR1 activity, and targeting Akt kinase/Akt phosphorylation (Li et al., 2018; Szliszka et al., 2009; Jing et al., 2010). Furthermore, it was reported that IBC could inhibit the proliferation of gastric cancer line (MGC803) through induction of apoptosis as well as inhibition of Akt and Erk signaling pathways (Jin and Shi, 2016). Zhang et al., also showed that IBC-induced cancer cell death is mediated by apoptosis- and
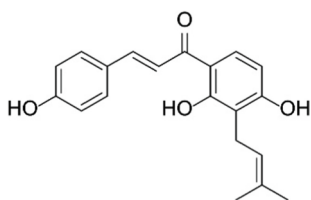
Scheme 1. The chemical structure of isobavachalcone (IBC).

autophagy-related pathways in human breast cancer MCF-7 cells (Zhang et al., 2022). Additionally, Wu et al., demonstrated that IBC might be able to mitigate glioblastoma cell proliferation and metastasis *in vitro* and *in vivo* without any remarkable adverse effects through mitochondria-dependent apoptosis (Wu et al., 2022).

Among the most frequently detected malignancies, colorectal cancer is one of leading cause of morbidity and death in China (Wang et al., 2023). Although different approaches including surgical resection, chemotherapy, radiotherapy, and immunotherapy are commonly recruited as therapeutic strategies for colorectal cancer, any of these therapies have not been able to provide us with an efficient therapeutic outcome (Simpson and Scholefield, 2008; Yang et al., 2023). Finding naturally occurring chemopreventive substances with low toxicity that can inhibit or reverse the multi-step carcinogenesis process has received a lot of attention recently (Ma et al., 2021; Singh et al., 2019).

Furthermore, it has been demonstrated that overexpression of survivin contributes significantly to the proliferation, metastasis, and resistance of cancer cells to therapeutic approaches (Li et al., 2018), which can be used as a potential target for tumor therapy (Garg et al., 2016). Survivin as a 16.5 kDa antiapoptotic protein consists of two N-terminal and C-terminal domains (Albadari and Li, 2023). The crystal structure shows a substantial dimerization interface along a hydrophobic patch on the N-terminal domain of each survivin. Therefore, functional protein–protein interaction plays a key role in fulfilling the antiapoptotic function of survivin (Albadari and Li, 2023; Verdecia et al., 2000). Based on these facts, developing some strategies in targeting survivin by small molecules can be recruited as a promising point for cancer therapy. Indeed, the potential interaction of IBC with survivin structure and amino acid residues involved in the dimerization process of survivin can inhibit the function of this protein as an antiapoptotic protein. Also, the majority of cancer cells express survivin at high levels, which inspired us to explore the novelty of this study as the inhibitory effect of IBC on the proliferation of metastatic colorectal cancer cell mediated by targeting survivin.

Therefore, in this study, the anticancer proprieties of IBC against human colorectal carcinoma Lovo cells were studied using different cellular and molecular techniques, while WI-38 human fibroblast cells were used as the normal cell line. Also, 5-Fluorouracil (5-FU) was used as a positive anticancer drug. Then, the interaction of IBC with survivin was analyzed by different spectroscopic measurements and theoretical analysis.

2. Materials and methods

2.1. Materials and cell culture

Isobavachalcone [CAT Nr: SML1450, ≥98 % (HPCE]), 5-FU (F6627-1G, purity ≥ 99 %), and 1-anilino-8-naphthalenesulfonic acid hemi-magnesium salt hydrate (ANS) were purchased from Sigma and were dissolved in dimethyl sulfoxide (DMSO) for experimental assays. Recombinant human survivin protein (142 amino acid range, >90 % purity) was obtained from AbCam (ab87202). The solutions containing survivin (5 μM) were prepared in 20 mM phosphate buffer solution (PBS) containing 100 mM NaCl and 50 μM Zn^{2+}, pH 8.0 (Gao et al., 2010). All of the other chemicals and reagents were from Sigma or Invitrogen.

2.2. Cell culture

Human colorectal carcinoma Lovo cells and WI-38 human fibroblast cells obtained from American Type Culture Collection (Manassas, VA, USA) were cultured in the F12 (Invitrogen, Carlsbad, CA, USA) and Dulbecco's modified Eagle's medium (DMEM/ Life Technologies), respectively containing 10 % FBS (fetal bovine serum, Invitrogen) and 1 % antibiotics (Sigma, USA) in a humidified atmosphere of 95 % air and 5 % CO_2 at 37 °C.

2.3. MTT assays

Cells (5×10^3) per well seeded in 96-well tissue culture plates were incubated overnight and media were then replaced with fresh ones containing increasing concentrations of IBC (0, 1, 10, 20, 30, 50, and 100 μM). After 24 h, MTT assay was performed by replacing the media with 1 mg/ml MTT solution and incubation for 4 h in the dark. MTT solution was then gently removed and the wells were added by 100 μl of DMSO. The optical density of samples was read using a Dynex Opsys MR ELISA plate reader (Worthing, West Sussex, UK) at 570 nm.

2.4. Lactate dehydrogenase (LDH) assay measurements

After overnight incubation of cells, media were replaced with fresh media containing increasing concentrations of IBC (0, 1, 10, 20, 30, 50, and 100 μM). After 24 h of incubation, fixed amounts of media were collected and immediately used for the LDH assay. LDH assays were measured using a LDH Assay Kit (Colorimetric, ab102526) according to the manufacturer's protocol. The optical density of samples was read using a Dynex Opsys MR ELISA plate reader (Worthing, West Sussex, UK) at 450 nm.

2.5. Determination of reactive oxygen species (ROS)

ROS generation was assessed using a DCFH-DA fluorescence assay. The treated cells were incubated with DCFH-DA (10 μM, sigma, USA) for 30 min at 37 °C. Then the cells were washed twice with PBS and the fluorescence intensity was determined at 525 nm (λex = 488 nm).

2.6. Determination of lipid peroxidation

The presence of malondialdehyde (MDA) was assessed using the TBARS Assay Kit (Thiobarbituric Acid Reactive Substances, Cayman Chemical, Michigan 48,108 USA) as described previously (Ni et al., 2019). Briefly, after treatment, the cells were homogenized, incubated with thiobarbituric acid reactive substances and the absorbance of samples was read using a Dynex Opsys MR ELISA plate reader (Worthing, West Sussex, UK) at 530–540 nm.

2.7. Superoxide dismutase (SOD) and catalase (CAT) activity and glutathione (GSH) content assays

The biochemical assays for SOD and CAT were performed to assess the endogenous antioxidant activity in LoVo cells. The cell suspension after treatment was processed for SOD and CAT activity assays. The antioxidant activity in LoVo cells was analyzed by determining the SOD and CAT based on the recommended protocols provided with SOD assay kit (ab65354) and CAT assay kit (ab83464). Determination of GSH content was also done based on the method reported previously by Beutler et al (Beutler et al., 1963) and updated by Gu et al. (Gu et al., 2015).

2.8. Quantitative real-time PCR (qTR-PCR) analysis

Total RNA content of the LoVo cells was isolated using a RNeasy® Mini Kit (QIAGEN, Hilden, Limburg, Germany) according to the

manufacturer's protocol. cDNA was synthesized using an RT-PCR kit (Takara, Kyoto, Japan). Real-time PCR was performed using SYBR Green Premix Ex Taq on an ABI ViiA 7DX RT-PCR machine. $2^{-\Delta\Delta ct}$ method was used for calculating the fold change and the primer sequences were used based on the previous papers reported by Afrin et al. and Zhang et al. (Afrin et al., 2018; Zhang et al., 2019).

2.9. Detection of mitochondrial membrane potential (MMP)

MMP assay was done with JC-1 staining as previously explained (Panada et al., 2023). Briefly, at 24 h after the IBC treatment (35 μM), LoVo cells were harvested and incubated with JC-1 at a final concentration of 2 μM at 37 °C in the dark for 15 min. The cells were then centrifuged, rinsed with HEPES buffer, resuspended, and MMP changes were assessed ratiometrically by determining the ratio of JC-1 fluorescence at 590 nm (red) and 530 nm (green) (λex = 490 nm).

2.10. Measurement of caspase-3 and −9 activity

Caspase-3 and caspase-9 activities were assessed using relevant kits according to the manufacturer's instructions (Beyotime Biotech, China). Briefly, LoVo cells (1×10^6) were treated with IC_{50} concentration of IBC (35 μM), harvested, washed twice with PBS, resuspended in lysis buffer, incubated on ice for 15 min, centrifuged at $18,000 \times g$ for 10 min at 4 °C, and exposed to caspase activity assay. Reaction buffer with substrates acetyl-Asp-Glu-Val-Asp-p-nitroanilide (Ac-DEVD-pNA, caspase-3) and acetyl-Leu-Glu-His-Asp-p-nitroanilide (Ac-LEHD-pNA, caspase-9), were used for detection of caspase activity. The pNA release was determined using a Dynex Opsys MR ELISA plate reader (Worthing, West Sussex, UK) at 405 nm.

2.11. Cytochrome c and survivin determination

ELISA kit (Abcam, Cambridge, UK) was used to analyze the release of apoptotic marker (Cyt C protein) and survivin protein expression according to the manufacturer's protocols. Briefly LoVo cells (5×10^5 cells) per well were treated with 35 μM IBC or 5-FU for 24 h. After harvesting, the cells were washed twice with ice-cold PBS, resuspended in cold lysis buffer for 30 min, and centrifuged at $12000 \times g$ for 15 min at 4 °C. Then, supernatants were collected and used for protein assay. The color was detected and quantified at 450 nm with a microplate reader (Worthing, West Sussex, UK).

2.12. Spectroscopic analysis

2.12.1. Intrinsic fluorescence measurement
The intrinsic fluorescence of survivin was read on a Cary Eclipse fluorescence spectrophotometer (Agilent, Santa Clara, California, USA) at four different temperatures of 298, 302, 310, and 315 K. Protein concentration was fixed at 3 μM and titrated with different concentrations of IBC ranging from 3 to 28.8 μM. The samples were excited at 295 nm, and the emission spectra were recorded from 290 to 450 nm. Both the excitation and emission slits were fixed at 5 nm. The fluorescence signals were corrected against the intrinsic fluorescence intensity of IBC and inner filter effects. All samples were prepared and equilibrated for 5 min.

2.12.2. ANS fluorescence measurement
The ANS fluorescence intensities of free survivin and survivin-IBC complex (molar ratios of 1:1, 1:5, and 1:10) at room temperatures were read at 480 nm by excitation of protein samples at 380 nm. The ANS concentration was 30 μM. All other experimental parameters were similar to the intrinsic fluorescence measurement section.

2.12.3. Circular dichroism (CD) spectroscopy
Far-UV CD spectra of free survivin (10 μM) and survivin-IBC complex

(molar ratios of 1:1, 1:5, and 1: 10) were read using a Jasco J-810 spectrophotometer (Tokyo, Japan) at room temperature using a 0.1 cm path length. The CD spectra of buffer and IBC solutions were subtracted from the protein CD spectra. All samples were prepared and equilibrated for 5 min and the measurement was performed at room temperature.

2.13. Molecular docking study

A molecular docking study was done using AutoDock software. The structure of IBC ($C_{20}H_{20}O_4$) was downloaded from PubChem (PubChem CID: 5281255) in a 3D conformer (SFD). Low energy 3D conformer of the IBC was docked with survivin protein (PDB ID: 3UIH). During the docking process, charge optimization, hydrogen atom addition and removal of water molecules were performed. The docking procedure was done based on the default settings. The blind docking was done within the survivin protein as a rigid receptor. The AutoDock scoring set was then used to score the resulting interactions and the molecular docking results were visualized by relevant software.

2.14. Statistical analyses

Data are represented as the average of three experiments and error bars represent the standard deviation. Statistical analysis was performed via one-way analysis of variance (ANOVA). $p < 0.05$ was considered to be statistically significant.

3. Results and discussion

3.1. Effects of IBC on the cell viability and membrane integrity

Fig. 1a displays that IBC reduced the proliferation of the human LoVo colorectal cancer cell based on a concentration-dependent manner, however, IBC did not significantly mitigate the growth of WI-38 normal cells up to 50 μM. Indeed, it was realized that upon incubation of the human LoVo colorectal cancer cell with 1, 10, 20, 30, 50, and 100 μM IBC, the cell viability was reduced from 100.00 % to 96.74 %, 83.19 %, 77.49 %, 48.92 %, 43.04 %, and 39.02 % respectively. While, the cell viability values were 100.00 %, 101.87 %, 94.37 %, 89.86 %, 88.39 %, and 80.44 % after incubation of WI-38 normal cells with 1, 10, 20, 30, 50, and 100 μM IBC at 24 h. Therefore, it was deduced that IBC at concentrations above 1 μM was able to significantly inhibit the proliferation of the human LoVo colorectal cancer cell, while it was only cytotoxic against WI-38 normal cells at a concentration of 100 μM.

Data are shown as mean ± SD ($n = 3$). * $p < 0.05$, * * $p < 0.01$, * ** $p < 0.001$.

Then the IC_{50} concentration of IBC against human LoVo colorectal cancer cells was determined to be approximately 35 μM. Li et al. (Li et al., 2019) showed that IC_{50} concentrations of IBC against HCT116 and SW480 colorectal cancer cells were 75.48 μM and 44.07 μM at 24 h, detected by CCK-8 assay. Furthermore, Table 1 shows the IC_{50} concentrations of IBC against different cancer cell lines.

Destruction of membrane leakage induced by bioactive compounds can be one of the possible mechanisms of their anticancer activity (Zhu et al., 2016; Fang et al., 2023). For this reason, we aimed to investigate the effect of IBC incubation on the membrane integrity of the human LoVo colorectal cancer cells and WI-38 normal cells. We found that IBC incubation above concentrations of 10 μM could result in the membrane leakage in LoVo colorectal cancer cells (Fig. 1b). However, the relative LDH release values in WI-38 normal cells following incubation with increasing concentrations of IBC remained unchanged in comparison with the control group (Fig. 1b), revealing the minimum damage to membrane integrity of normal cells.

3.2. IBC increased intracellular oxidative stress

Oxidative stress is a crucial factor that mediates the bioactive
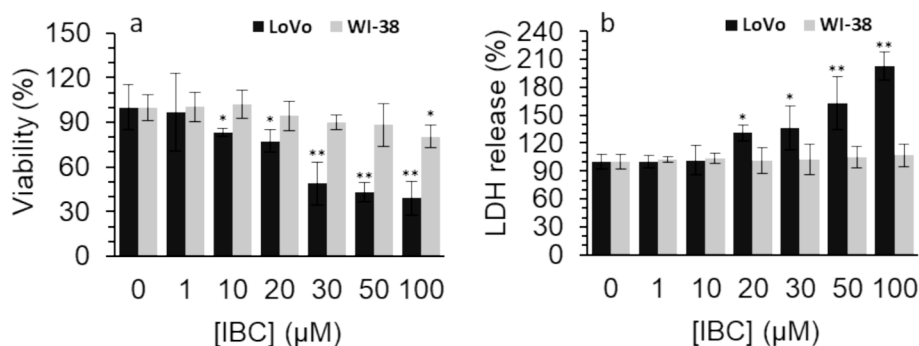
Fig. 1. (a) Effect of different concentrations of IBC on the viability of the LoVo cancer and WI-38 normal cells after 24 h assessed by MTT assay. (b) Effect of different concentrations of IBC on membrane damage of the LoVo cancer and WI-38 normal cells after 24 h assessed by LDH assay.

Table 1
The IC_{50} concentration of IBC against different cancer types.

Cancer cells	Cell line(s)	Time (h)	IC_{50} (μM)	Ref(s).
Leukemia	NB4, U937, K562s, K562r	24–42	< 20	(Yang et al., 2019; Li-li et al., 2014; Wu et al., 2018)
Colorectal cancer	HCT116, SW480	24	44.07 and 75.48	(Li et al., 2019)
Gastric cancer	MGC803	24 and 48	49.68 ± 4.26 and 39.96 ± 3.78 μM	(Jin and Shi, 2016)
liver cancer	HepG2 and Hep3B	48	16.45 and 13.22	(Li et al., 2019)
Cervical cancer	HeLa	24	> 50	(Szliszka et al., 2012)
Breast cancer	MCF-7	24, 48, and 72	38.46, 31.31, and 28.26	(Zhang et al., 2022)
Breast cancer	MDA-MB-231	24, 48, and 72	21.45, 15.15, and 8.53	(Wu et al., 2022)
Tongue	Tca8113	24	128. 31 ± 6. 83	(Shi et., et al., 2015; Shi et al., 2017)
Colorectal	LoVo	24	35	This study

compounds-induced anticancer effects. For example, Li et al. (Li et al., 2018) showed that IBC stimulated oxidative stress-mediated cell death by targeting antioxidant enzymes in human prostate cancer PC-3 cells. Also, He et al. reported that IBC prohibits acute myeloid leukemia, where oxidative stress through excessive ROS generation resulted in mitochondrial apoptosis (He et al., 2021). Furthermore, Zhao et al. (Zhao et al., 2022) displayed that IBC can disrupt mitochondrial respiration and stimulate cytotoxicity mediated by ROS generation. Excessive ROS generation and lipid peroxidation products have been shown to play a key role in the prevention of cancer progression and therapy

(Barrera, 2012). Oxidative stress is a process by which a high intracellular ROS generation could destroy the lipids, proteins, and DNA structures (Chiang et al., 2022). Also, oxidative stress could be related to a variety of pathological factors (Chiang et al., 2022). This study showed that IBC could result in the production of excessive ROS in the human LoVo colorectal cancer cells ($P < 0.01$, Fig. 2a). In other words, when human LoVo colorectal cancer cells were exposed to 35 μM IBC for 24 h, the DCF fluorescence intensity level increased remarkably due to the formation of ROS.

MDA is considered the main product of lipid peroxidation which prompts cytotoxicity in different cells (Niedernhofer et al., 2003). This study showed that IBC could give rise to elevation of MDA level in the human LoVo colorectal cancer cells (Fig. 2b). When the human LoVo colorectal cancer cells were incubated with 35 μM IBC for 24 h, the produced MDA level increased significantly. However, in both cases the effect of 5-FU as positive control was much higher in induction of oxidative stress in the human LoVo colorectal cancer cells than IBC-treated cells.

Both antioxidant enzymes, SOD and CAT, as well as non-enzyme antioxidant substance, GSH, are considered the key modulators in the regulation of oxidative stress (Gu et al., 2015; Jelic et al., 2021). Our data showed that SOD activity (Fig. 3a) and CAT activity (Fig. 3b) were significantly reduced by both IBC and 5-FU, further revealing that IBC may degrade or inactive SOD and CAT in the human LoVo colorectal cancer cells.

Additionally, intracellular GSH as the crucial non-enzymatic antioxidant system could serve as a free radical scavenger molecule to shield cells in response to oxidative stress (Estrela et al., 2006; Marini et al., 2023). We showed that both IBC and 5-FU reduced the content of GSH (Fig. 3c), indicating that IBC might be able to alter the redox status and consequently induce a high level of oxidative stress.

Together, these data suggested that IBC could elevate the level of oxidative stress in the human LoVo colorectal cancer cells, which may
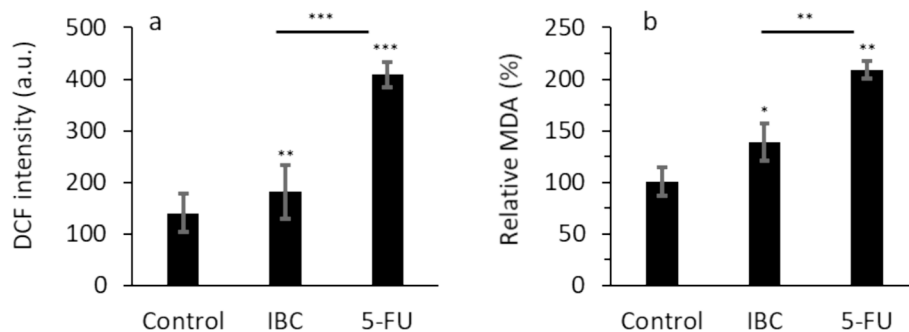
Fig. 2. (a) Effect of IC_{50} concentration of IBC (35 μM) or 35 μM 5-FU on DCF intensity (ROS formation) of the LoVo cancer cells after 24 h. (b) Effect of IC_{50} concentration of IBC (35 μM) or 35 μM 5-FU on MDA level of the LoVo cancer cells after 24 h. Data are shown as mean ± SD ($n = 3$). * $p < 0.05$, ** $p < 0.01$, *** $p < 0.001$.
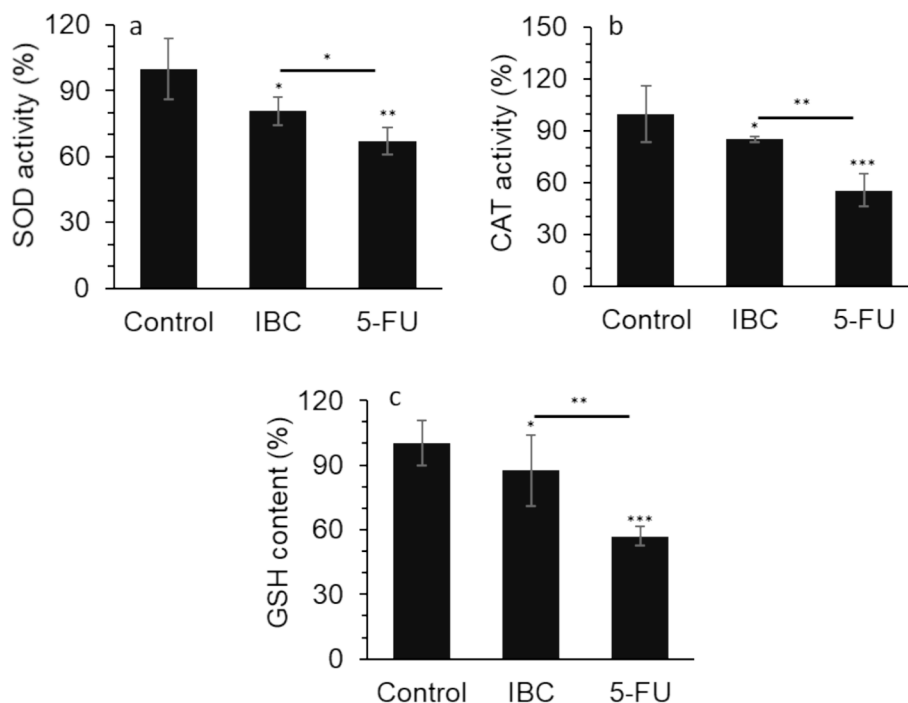
Fig. 3. (a) Effect of IC_{50} concentration of IBC (35 μM) or 35 μM 5-FU on SOD activity of the LoVo cancer cells after 24 h. (b) Effect of IC_{50} concentration of IBC (35 μM) or 35 μM 5-FU on CAT activity of the LoVo cancer cells after 24 h. (c) Effect of IC_{50} concentration of IBC (35 μM) or 35 μM 5-FU on GSH content of the LoVo cancer cells after 24 h. Data are shown as mean ± SD ($n = 3$). * $p < 0.05$, ** $p < 0.01$, *** $p < 0.001$.

further cause increased cell death. More importantly, these data may suggest that incubation of the LoVo cancer cells with the IBC can be a potential strategy to deregulate oxidative/antioxidant balance in cancer cells as a main mechanism for the induction of anticancer effects.

3.3. IBC decreased expression of Nrf2 and HO-1 in LoVo cells

Nrf2 as a potential antioxidant pathway can protect cells against oxidative stress-mediated damage, indicating that this pathway could induce resistance to cancer therapy (Gallorini et al., 2023). Nrf2 could modulate several important molecules in antioxidant systems including CAT, SOD, and GSH (Liang et al., 2018). SOD, CAT and GSH could prevent cell apoptosis caused by free radicals (Liang et al., 2018). HO-1 is known as an antioxidative protein which is modulated by the Nrf2 as a transcription factor (Ghareghomi et al., 2023).

This study revealed that both Nrf2 (Fig. 4a) and HO-1 (Fig. 4b) expression at the mRNA level were downregulated significantly when the human LoVo colorectal cancer cells were treated with 35 μM IBC for 24 h.

Kim et al. (Kim et al., 2020) reported that Nrf2 knockdown could result in re-sensitization of pancreatic cancer cells to 5-FU resistance through suppressing HO-1 expression. Also, Kweon et al. (Kweon et al., 2006) demonstrated that Nrf2-mediated overexpression of HO-1 plays a key role in resistance to apoptosis in human lung cancer cells induced by epigallocatechin 3-gallate. We then, demonstrated that IBC promotes oxidative stress in the human LoVo colorectal cancer cells via Nrf2/HO-1 signaling pathway, which is in good agreement with previous studies (Wei et al., 2021; Acquaviva et al., 2021).

3.4. IBC triggered mitochondrial dysfunction, release of cytochrome c, and activation of apoptosis in LoVo cells

The importance of mitochondrial dysfunction in cancer therapy has been widely reported in the literature (Luo et al., 2020; Księżakowska-Łakoma et al., 2014). Also, Cyt C is placed in the mitochondrial inter-membrane/intercristal spaces and serves as an electron shuttle molecule in the respiratory chain. Different proapoptotic encouraging signals (Bcl-2-like proteins) promote the permeabilization of the outer
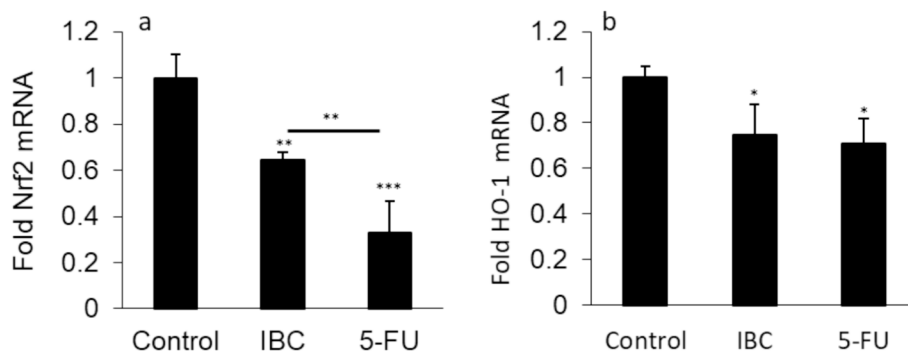
Fig. 4. (a) Effect of IC_{50} concentration of IBC (35 μM) or 35 μM 5-FU on expression of Nrf2 mRNA of the LoVo cancer cells after 24 h. (b) Effect of IC_{50} concentration of IBC (35 μM) or 35 μM 5-FU on expression of HO-1 mRNA of the LoVo cancer cells after 24 h. Data are shown as mean ± SD ($n = 3$). * $p < 0.05$, ** $p < 0.01$, *** $p < 0.001$.

membrane, mediate the interaction between intermembrane and inter-cristal spaces and assist the Cyt C release to the cytosol (Garrido et al., 2006; Hussar, 2022). Then, Cyt C promotes the activation of several mechanisms which are the main activator of caspase-9 and caspase-3. Activated caspases finally result in the induction of apoptosis. The caspase overactivation associated with the release of Cyt C to cytoplasm can be inhibited by Bcl-2 overexpression or Bax downregulation. Indeed, the Bcl-2 family (BCL-XL, MCL-1, BAK, BOK, BAD, BID, BIM) regulates MMP. These molecules could interact with each other to result in the formation of homo/hetero-complexes and play a key role in regulating

MMP and prevention of apoptosis (Garrido et al., 2006; Hussar, 2022).

Therefore, in this study, the effects of IBC on the mitochondria destruction, release of Cyt C, Bax/Bcl-2 and caspase expression, and caspase activity in the human LoVo colorectal cancer cells were evaluated by relevant methods/techniques described in section 2.

Mitochondrial destruction is associated with alterations in MMP. Mitochondrial depolarization can be tracked by a reduction in the red/green fluorescence intensity ratio of JC-1 as a probe (Chiang et al., 2022). When the LoVo cells were subjected to IBC, the red/green fluorescence intensity ratio of JC-1 dye reduced significantly at 35 μM
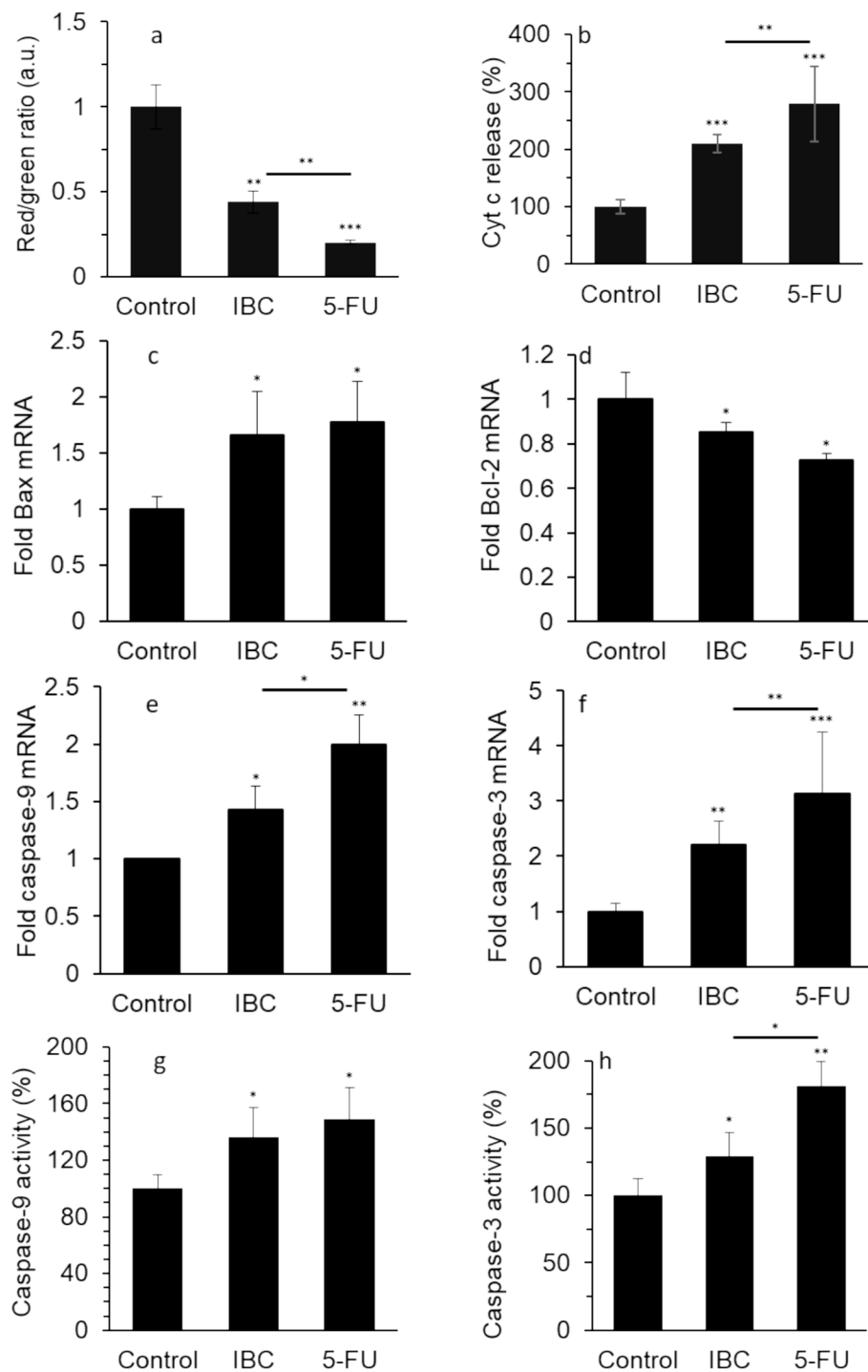
Fig. 5. Effect of IC$_{50}$ concentration of IBC (35 μM) or 35 μM 5-FU on (a) MMP loss, (b) release of Cyt c, (c) expression of Bax mRNA, (d) expression of Bcl-2 mRNA, (e) expression of caspase-9 mRNA, (f) expression of caspase-3 mRNA, (g) caspase-9 activity, and (h) caspase-3 activity of the LoVo cancer cells after 24 h. Data are shown as mean ± SD ($n = 3$). * $p < 0.05$, ** $p < 0.01$, *** $p < 0.001$.

(Fig. 5a). As already discussed, when healthy cells are exposed to extracellular or intracellular anticancer stimuli, the MMP reduced, and Cyt C is released from mitochondria into the cytoplasm (Chiang et al., 2022). When the human LoVo colorectal cancer cells were incubated with 35 μM IBC for 24 h, the Cyt C release in the cytoplasm was enhanced significantly (Fig. 5b).

As the Bcl-2 family plays a distinctive role in cell viability and apoptosis through the mitochondrial pathway, we aimed to devalue the effect of IBC on the expression level of Bcl-2 and Bax mRNA in the human LoVo colorectal cancer cells. This study showed that when the LoVo cells were subjected to 35 μM IBC for 24 h, the mRNA expression of Bax increased remarkably (Fig. 5c) but the mRNA expression of Bcl-2 decreased significantly (Fig. 5d). The same mRNA expression pattern was also detected for 5-FU (35 μM)-exposed LoVo cells for 24 h (Fig. 5c, d).

Apoptosis through the mitochondrial pathway is mainly modulated by the caspase-9 and −3. This study further explored whether IBC influenced the expression and activity of caspase-9 and −3 in the human LoVo colorectal cancer cells. When the LoVo cells were incubated with the IBC for 24 h, the caspase-9 mRNA expression (Fig. 5e), caspase-3 mRNA expression (Fig. 5f), caspase-9 activity (Fig. 5g), and caspase-3 activity (Fig. 5h) increased as the IBC concentration was 35 μM, which was also observed upon incubation of cells with 5-FU with the similar experimental procedure.

3.5. IBC downregulated the expression of survivin in LoVo cells

The antiapoptotic survivin is known as one of the main inhibitors of apoptosis, which is overexpressed particularly in cancer cells and increases the survival rate of cancer cells mediated by downregulation of caspase-linked apoptosis (Touloumis et al., 2020; Sabour et al., 2020). Upregulation of survivin is directly correlated with cancer cell proliferation, invasion and resistance and poor patient prognosis which necessitate the development of new and potential therapeutic approaches involving survivin targeting in cancer (Martínez-García et al., 2019). By searching the literature for IBC as an effective inhibitor of survivin, we found that IBC has been shown to have a significant effect on survivin expression (Li et al., 2019). We then aimed to determine whether IBC (35 μM) at 24 h leads to survivin downregulation and degradation in the human LoVo colorectal cancer cells as a metastatic cell model. As shown in Fig. 6, IBC similar to 5-FU significantly inhibited survivin expression at both mRNA (Fig. 6a) and protein (Fig. 6b) levels in LoVo colorectal cancer cells at a concentration of 35 μM.

This data indicated that IBC might induce apoptosis in LoVo cells through downregulation of antiapoptotic (survivin, Bcl-2) and upregulation of apoptotic (Bax, caspase, Cyt C) factors, which these data are in line with findings reported by Li et al (Li et al., 2019).
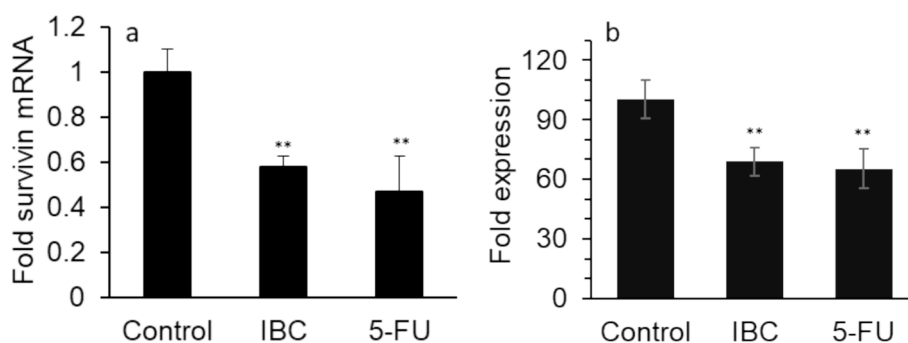
3.6. Interaction properties of IBC and survivin

The intrinsic fluorescence of survivin arising from tryptophan residues can be used as a very important indicator of conformation alterations (dos Santos Rodrigues et al., 2023; Kyrychenko and Ladokhin, 2024). As shown in Fig. 7, when excited at 295 nm, the free survivin sample demonstrated the maximum emission intensity (λ_{max}) around 341 nm at all four studied temperatures (Fig. 7a-d). However, remarkable differences were detected in fluorescence intensity at λ_{max} following increasing the IBC in a concentration-dependent manner.

These phenomena revealed that there were some structural changes and exposed hydrophobic moieties on the survivin-IBC complex (dos Santos Rodrigues et al., 2023). Similar phenomena in quenching of fluorescence intensity were also observed for bile salt hydrolases after interaction with IBC (Li et al., 2022). This might be associated with the partial unfolding of proteins occurring following interaction (Gooran and Kopra, 2024). These conformation changes could lead to displacement and masking of Trp residues or exposure to a polar environment (Gooran and Kopra, 2024).

3.6.1. Fluorescence quenching mechanism

Generally, static and dynamic quenching caused by complex formation (strong) and collision (weak), respectively can be distinguished by the Stern-Volmer Equation (Kenoth and Kamlekar, 2022):

$$F_0/F = 1 + K_{SV}[IBC] = 1 + kq\tau_0[IBC] \qquad (1)$$

where F_0 and F, [IBC], K_{SV}, k_q, and τ_0 are the fluorescence intensities of survivin in the absence of the quencher (here, IBC), the fluorescence intensities of survivin in the presence of the IBC, concentration of IBC, Stern-Volmer quenching constant, the quenching rate constant, and the average lifetime of the free proteins (10^{-9} s), respectively.

Stern-Volmer plots in Fig. 8a show good linearity at the four different temperatures studied, indicating that almost one type of quenching mechanism is involved in the survivin-IBC interaction (Khalil and Kashif, 2023; Sun et al., 2024; Yi et al., 2024).

The quenching parameters are summarized in Table 2.

The data in Table 2 showed that quenching parameters increase with an elevation of temperature, while k_q values are much greater than $1 \times 10^{10}\ \mathrm{M}^{-1}\ \mathrm{s}^{-1}$. In particular, k_q values play a key role in dictating the type of quenching mechanism occurring following the interaction of protein and ligands (Sun et al., 2024). For the dynamic quenching mechanism, the k_q values are close to the diffusion-controlled limit ($1 \times 10^{10}\ \mathrm{M}^{-1}\ \mathrm{s}^{-1}$), while higher k_q values reflect the contribution of static quenching (Sun et al., 2024). In the present study, k_q values are 3 orders of magnitude higher than the diffusion-controlled limit ($1 \times 10^{10}\ \mathrm{M}^{-1}\ \mathrm{s}^{-1}$), indicating that the survivin-IBC interaction is mostly static in nature. Similar findings have been reported in the interactions of IBC with bile salt hydrolases (Li et al., 2022).

Fig. 6. Effect of IC$_{50}$ concentration of IBC (35 μM) or 35 μM 5-FU on (a) expression of survivin mRNA and (b) expression of survivin protein of the LoVo cancer cells after 24 h. Data are shown as mean ± SD ($n = 3$). ** $p < 0.01$.
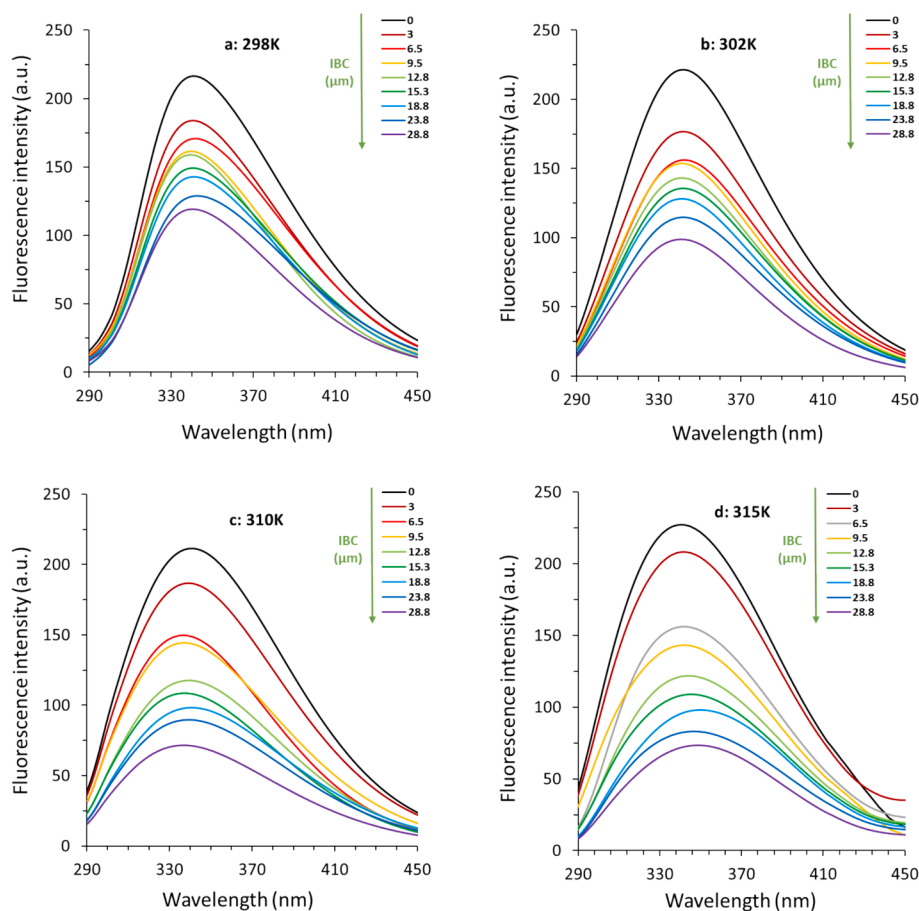
Fig. 7. Effect of various concentrations of IBC on fluorescence quenching of survivin at four different temperatures of (a) 298 K, (b) 302 K, (c) 310 K, and (d) 315 K.

3.6.2. Evaluation of binding parameters

For a static quenching mechanism, the binding constant (K_b) and the numbers of binding sites (n) can be determined using the following double-log Equation (Sun et al., 2024):

$$\log F_0 - F/F = n\log K_b + nLog([IBC_t] - [P_t]F_0 - F/F_0) \tag{2}$$

where [P_t] is the total protein concentration. The rest of parameters are similar to Equation (1). The plots of $\log(F_0$-F)/F versus log(($[Q_t]$-[P_t](F_0-F)/F_0)) for the survivin-IBC system at four different temperatures are shown in Fig. 8b, and the calculated parameters are presented in Table 3.

As tabulated in Table 3, the magnitude orders of K_b values of survivin-IBC complex are in the range of 10^2-10^6 mol^{-1}, which suggests a strong affinity between IBC and survivin at physiological temperature (315 K) (Zhao et al., 2022). In fact, K_b value of IBC at 315 K is higher than that in lower temperatures, implying that IBC has a greater affinity to survivin at higher temperatures. This phenomenon is may be caused by slight structural changes in survivin at higher temperatures, which favor survivin–IBC interaction. Similar outcomes are also detected for the interaction of IBC with bile salt hydrolases (Li et al., 2022).

Furthermore, the variations of the n increase with elevating temperature for survivin–IBC interaction, revealing the heat-induced slight conformational changes of protein and possible favorable interaction of IBC and survivin (Roslan and Tayyab, 2019; Li et al., 2022; Siddiqui et al., 2021).

3.6.3. Evaluation of thermodynamic parameters

Moreover, the K_b values are employed to determine the thermodynamic parameters (Table 4), enthalpy change (ΔH) and entropy change (ΔS) by the well-known Van't Hoff Equation (Sun et al., 2024):

$$LnK_b = \Delta H/RT + \Delta S/R \tag{3}$$

where, R and T are gas constant and temperature, respectively, and the plots are given in Fig. 8c.

Gibbs free energy change (ΔG) can be determined by using the following Equation (Sun et al., 2024):

$$\Delta G = \Delta H - T\Delta S = -RTlnK_b$$

In general, positive ΔH and ΔS values indicated the presence of hydrophobic forces (Sun et al., 2024; Siddiqui et al., 2021). Also, negative ΔG values indicated that the reaction of survivin-IBC complex formation is spontaneous. These calculated thermodynamic parameters (Table 3) specified that the binding process for survivin-IBC complex was spontaneously driven by ΔS and considerably mediated by hydrophobic interactions (Sun et al., 2024).

3.7. Effect of IBC on survivin structure

The surface hydrophobicity of proteins can be determined using ANS fluorescence spectroscopy (Togashi and Ryder, 2008). ANS acts as an extrinsic fluorescent dye which is exceedingly sensitive to microenvironmental changes (Tang et al., 2020). ANS quantum yield extremely increases upon interaction with hydrophobic groups of proteins (Guliyeva and Gasymov, 2020). Therefore, ANS fluorescence spectroscopy may be used for detecting probable modifications in protein surface hydrophobicity triggered by drug/ligand binding. At a fixed concentration of survivin (3 μM) and ANS (30 μM), ANS fluorescence intensities were detected in the absence and presence of varying concentrations of IBC (Fig. 9a).

A significant increase in the ANS fluorescence intensity was observed
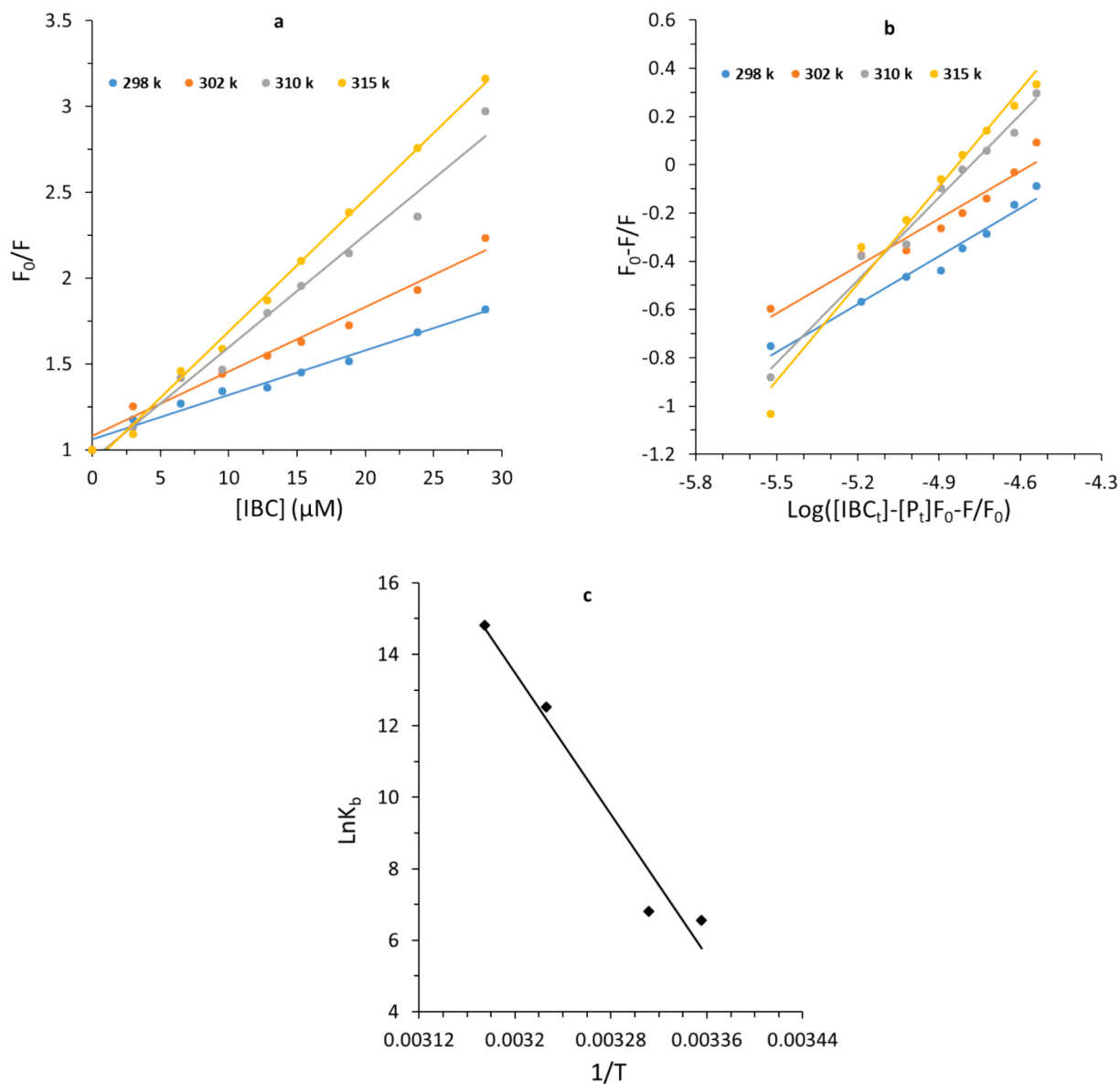
Fig. 8. (a) Stern-Volmer plots, (b) modified stern-Volmer plots, and (c) Van't Hoff plots of survivin-IBC complex.

Table 2
Quenching parameters for the interaction of survivin with IBC at four different temperatures.

T (K)	K_{SV} ($\times 10^4$ mol^{-1})	k_q ($\times 10^{13}$ mol^{-1}s^{-1})	R^2[a]
298	2.60	2.60	0.98
302	3.76	3.76	0.97
310	6.54	6.54	0.98
315	7.71	7.71	0.99

[a] R^2 is the correlation coefficient.

Table 3
Binding parameters for the interaction of survivin with IBC at four different temperatures.

T (K)	$\log K_b$	n	R^2[a]
298	2.85	0.65	0.97
302	2.96	0.65	0.95
310	5.45	1.14	0.98
315	6.44	1.33	0.97

[a] R^2 is the correlation coefficient.

Table 4
Thermodynamic parameters for the interaction of survivin with IBC at four different temperatures.

T (K)	ΔH (kJ/mol)	$T\Delta S$ (kJ/mol)	ΔG (kJ/mol)	ΔG (lnK_b)
298	411.98	426.24	−14.25	−16.21
302	411.98	431.96	−19.97	−17.06
310	411.98	443.40	−31.41	−32.25
315	411.98	450.55	−38.56	−38.72

upon increasing the IBC to the protein sample, which demonstrates the increase in the surface hydrophobicity of survivin. Indeed, the ANS fluorescence intensity of survivin in the absence of IBC is remarkably different in comparison to the presence of the IBC, which shows that the surface hydrophobicity of survivin is increased upon IBC binding.

CD spectroscopy measurement is used as a sensitive technique for recording the anticipated secondary structural changes of proteins upon ligand binding (Miles et al., 2021; Haque et al., 2022). Far-UV CD was then utilized to study the effect of IBC binding on survivin secondary structure. The far-UV CD spectra of survivin without and with varying
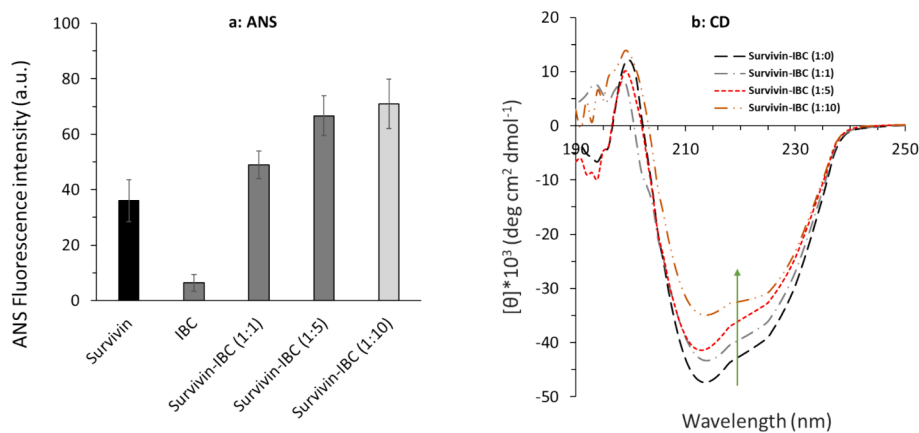
Fig. 9. (a) ANS fluorescence spectroscopy, and (b) far-UV CD spectroscopy measurements of survivin-IBC complex.

concentrations of IBC are exhibited in Fig. 9b. The results showed that the ellipticity changes around 222 and 208 nm, as an indicator of α-helicity content (Haque et al., 2022), decreased for the survivin in the presence of IBC in a concentration-dependent manner. Thus, it can be concluded that IBC binding to survivin caused a reduction in the survivin α-helicity content. All these data indicated that IBC resulted in survivin structural changes accompanied by microenvironmental changes around Trp residues, an increase of surface hydrophobicity, and a decrease of α-helicity content.

3.8. IBC potential interaction with survivin evidenced by molecular docking study

Survivin with a homodimer structure plays a key role in the

physiological function of cells (Sabour et al., 2020). Destabilization of the survivin following interaction with therapeutic small molecule into a domain that interferes with the dimerization hydrophobic interface, thereby further leading to cancer cell apoptosis.

To further provide insights on the obtained experimental results, IBC interaction with survivin was evaluated by theoretical study (Fig. 10). In this study, the IBC-survivin interactions were investigated by performing a molecular docking study using AutoDock software. The crystal structures of the IBC (Fig. 10a) and IBC-survivin complex (Fig. 10b) are shown in Fig. 10.

A docking study of IBC (Fig. 10b) showed that this compound was able to fit close to the binding pocket of survivin with a strong binding interaction with binding energy −9.80 kcal/mol (−41.00 kJ/mol). However, the binding energy of 5-FU with survivin was determined to be
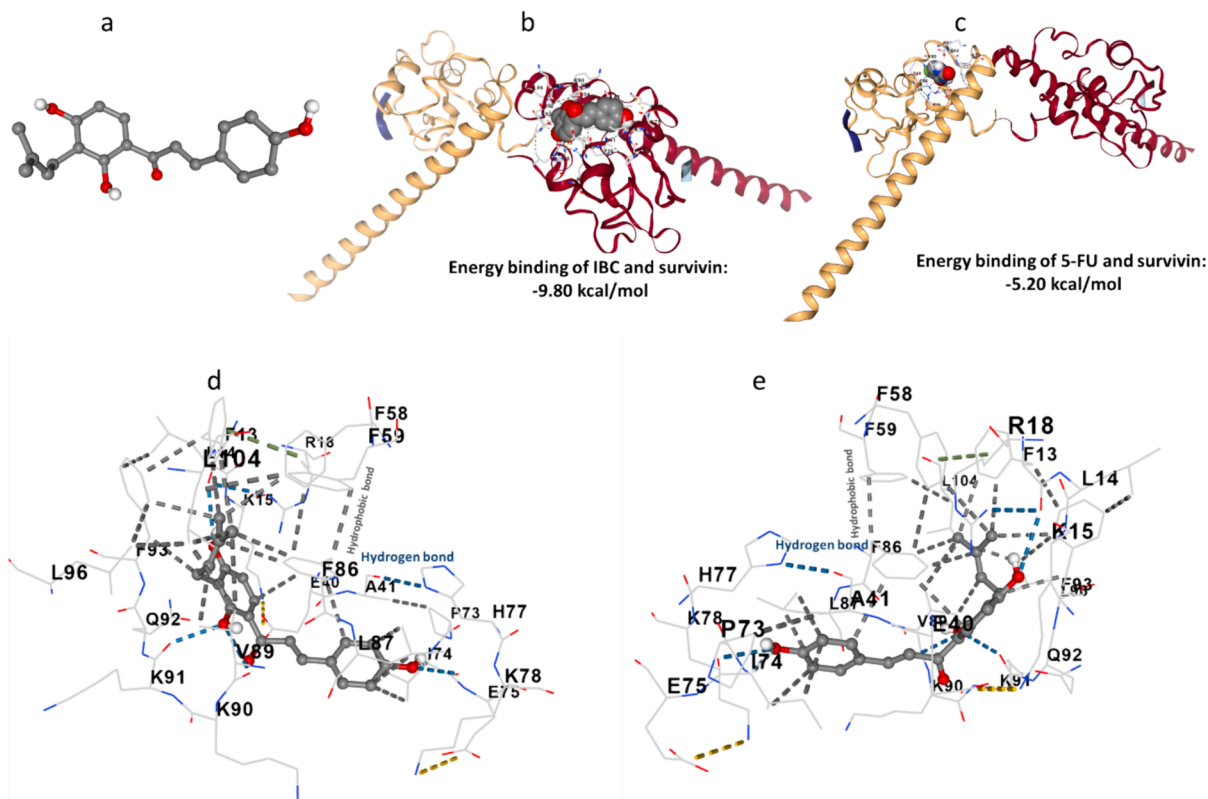
Fig. 10. (a) IBC structure, (b) binding of IBC and survivin, (c) binding of 5-FU and survivin, (d), binding pocket of IBC-survivin, and (e) binding pocket of 5-FU-survivin.

about −5.20 kcal/mol (−21.75 kJ/mol, Fig. 10c), revealing the higher affinity of IBC to survivin in comparison with 5-FU. It was then observed that hydrogen bonding between IBC and survivin was derived from the interaction of the Phe 13 and Lys91 with the IBC backbone (Fig. 10d, e). Also, Ile74, Phe86, Leu87, Val89, and Phe93 contributed to the formation of hydrophobic forces between IBC and survivin (Fig. 10 d, e), which is in good agreement with thermodynamic parameters determined by fluorescence quenching study.

Drawing from theoretical study, we can assert that IBC interacts with a survivin domain that plays a crucial role in the dimerization process. This compound can obstruct the dimerization hydrophobic interface, ultimately contributing to the apoptosis of cancer cells. This data is in good agreement with our experimental results and the finding reported by Sabour et al. which screened several cyanopyridine derivatives as survivin inhibitors by molecular docking study (Sabour et al., 2020).

4. Conclusion

In conclusion, we found that IBC could induce anticancer effects against human LoVo colorectal cancer cells, while it had minimum cytotoxicity against and normal cell line, WI-38. It was shown that IBC induced its anticancer effects through elevation of oxidative stress mediated by the deregulation of enzymatic and non-enzymatic antioxidant systems as well as downregulation of the Nrf2/HO-1 signaling pathway. Furthermore, incubation of the human LoVo colorectal cancer cells with the IBC at 24 h led to a remarkable induction of apoptosis through the mitochondrial pathway and reduction of survivin expression. Finally, it was observed that IBC via hydrogen bonding and hydrophobic forces interacted strongly with survivin in the vicinity of the dimerization domain, which might result in the conformational changes and destabilization of survivin. Therefore, we concluded that IBC might be recruited as a potential anticancer compound in future studies, although further *in vivo* and clinical studies are required to ascertain IBC's biomedical properties and ongoing limitations of this study.

CRediT authorship contribution statement

Li Zhang: Conceptualization, Methodology, Visualization, Formal analysis, Investigation, Software, Writing – original draft, Writing – review & editing. **Bo Yi:** Conceptualization, Methodology, Visualization, Formal analysis, Investigation, Software, Writing – original draft, Writing – review & editing. **Jing Chen:** Supervision, Data curation, Conceptualization, Visualization, Formal analysis, Investigation, Funding acquisition, Resources, Software, Writing – original draft, Writing – review & editing.

Declaration of competing interest

The authors declare that they have no known competing financial interests or personal relationships that could have appeared to influence the work reported in this paper.

References

Acquaviva, R., et al., 2021. Protocatechuic acid, a simple plant secondary metabolite, induced apoptosis by promoting oxidative stress through HO-1 downregulation and p21 upregulation in colon cancer cells. Biomolecules 11 (10), 1485.

Afrin, S., et al., 2018. Manuka honey synergistically enhances the chemopreventive effect of 5-fluorouracil on human colon cancer cells by inducing oxidative stress and apoptosis, altering metabolic phenotypes and suppressing metastasis ability. Free Radic. Biol. Med. 126, 41–54.

Albadari, N., Li, W., 2023. Survivin small molecules inhibitors: recent advances and challenges. Molecules 28 (3), 1376.

Barrera, G., 2012. Oxidative stress and lipid peroxidation products in cancer progression and therapy. Int. Scholar. Res. Notices 2012.

Beutler, E., Duron, O., Kelly, B.M., 1963. Improved method for the determination of blood glutathione. J. Lab. Clin. Med. 61, 882–888.

Bhalla, V.K., Nayak, U.R., Dev, S., 1968. Some new flavonoids from Psoralea corylifolia. Tetrahedron Lett. 9 (20), 2401–2406.

Chen, L., et al., 2023. Psoralea corylifolia L.: a comprehensive review of its botany, traditional uses, phytochemistry, pharmacology, toxicology, quality control and pharmacokinetics. Chin. Med. 18 (1), 1–38.

Chiang, Y.W., et al., 2022. Bisphenol A induced apoptosis via oxidative stress generation involved Nrf2/HO-1 pathway and mitochondrial dependent pathways in human retinal pigment epithelium (ARPE-19) cells. Environ. Toxicol. 37 (1), 131–141.

dos Santos Rodrigues, F.H., et al., 2023. Applications of fluorescence spectroscopy in protein conformational changes and intermolecular contacts. BBA Advances 3, 100091.

Estrela, J.M., Ortega, A., Obrador, E., 2006. Glutathione in cancer biology and therapy. Crit. Rev. Clin. Lab. Sci. 43 (2), 143–181.

Fang, X., et al., 2023. Pharmacokinetic investigation on the mechanism of interaction of anti-breast cancer calycosin with albumin: In vitro. Arab. J. Chem. 16 (10), 105175.

Gallorini, M., et al., 2023. Modulation of NRF2: biological dualism in cancer, targets and possible therapeutic applications. Antioxid. Redox Signal.

Gao, Y., et al., 2010. N-terminal deletion effects of human survivin on dimerization and binding to Smac/DIABLO in vitro. J. Phys. Chem. B 114 (47), 15656–15662.

Garg, H., et al., 2016. Survivin: A unique target for tumor therapy. Cancer Cell Int. 16 (1), 1–14.

Garrido, C., et al., 2006. Mechanisms of cytochrome c release from mitochondria. Cell Death Differ. 13 (9), 1423–1433.

Ghareghomi, S., et al., 2023. Modulation of Nrf2/HO-1 by natural compounds in lung cancer. Antioxidants 12 (3), 735.

Gooran, N., Kopra, K., 2024. Fluorescence-based protein stability monitoring—A review. Int. J. Mol. Sci. 25 (3), 1764.

Gu, S., et al., 2015. Resveratrol synergistically triggers apoptotic cell death with arsenic trioxide via oxidative stress in human lung adenocarcinoma A549 cells. Biol. Trace Elem. Res. 163, 112–123.

Guliyeva, A.J., Gasymov, O.K., 2020. ANS fluorescence: Potential to discriminate hydrophobic sites of proteins in solid states. Biochem. Biophys. Rep. 24, 100843.

Haque, M.A., et al., Application of circular dichroism spectroscopy in studying protein folding, stability, and interaction, in Advances in Protein Molecular and Structural Biology Methods. 2022, Elsevier. p. 213-224.

He, H., et al., 2021. Isobavachalcone inhibits acute myeloid leukemia: Potential role for ROS-dependent mitochondrial apoptosis and differentiation. Phytother. Res. 35 (6), 3337–3350.

Hussar, P., 2022. Apoptosis regulators bcl-2 and caspase-3. Encyclopedia 2 (4), 1624–1636.

Jelic, M.D., et al., 2021. Oxidative stress and its role in cancer. J. Cancer Res. Ther. 17 (1), 22–28.

Jiangning, G., et al., 2005. Antioxidants from a Chinese medicinal herb–Psoralea corylifolia L. Food Chem. 91 (2), 287–292.

Jin, X., Shi, Y.I., 2016. Isobavachalcone induces the apoptosis of gastric cancer cells via inhibition of the Akt and Erk pathways. Exp. Ther. Med. 11 (2), 403–408.

Jing, H., et al., 2010. Abrogation of Akt signaling by Isobavachalcone contributes to its anti-proliferative effects towards human cancer cells. Cancer Lett. 294 (2), 167–177.

Kenoth, R. and R.K. Kamlekar, Steady-state fluorescence spectroscopy as a tool to monitor protein/ligand interactions, in Optical Spectroscopic and Microscopic Techniques: Analysis of Biological Molecules. 2022, Springer. p. 35-54.

Khalil, A., Kashif, M., 2023. Interaction studies of levofloxacin with human lysozyme in a ternary complex using multispectroscopic and computational analysis: A circular dichroism method for the quantitation of levofloxacin. J. Mol. Liq. 370, 121023.

Kim, E.J., et al., 2020. NRF2 knockdown resensitizes 5-fluorouracil-resistant pancreatic cancer cells by suppressing HO-1 and ABCG2 expression. Int. J. Mol. Sci. 21 (13), 4646.

Księżakowska-Łakoma, K., Żyła, M., Wilczyński, J.R., 2014. Mitochondrial dysfunction in cancer. Menopause Review/przegląd Menopauzalny 13 (2), 136–144.

Kweon, M.-H., et al., 2006. Constitutive overexpression of Nrf2-dependent heme oxygenase-1 in A549 cells contributes to resistance to apoptosis induced by epigallocatechin 3-gallate. J. Biol. Chem. 281 (44), 33761–33772.

Kyrychenko, A., Ladokhin, A.S., 2024. Fluorescent probes and quenchers in studies of protein folding and protein-lipid interactions. Chem. Rec. 24 (2), e202300232.

Li, K., et al., 2018. Isobavachalcone induces ROS-mediated apoptosis via targeting thioredoxin reductase 1 in human prostate cancer PC-3 cells. Oxid. Med. Cell. Longev. 2018.

Li, Y., et al., 2019. Isobavachalcone isolated from Psoralea corylifolia inhibits cell proliferation and induces apoptosis via inhibiting the AKT/GSK-3β/β-catenin pathway in colorectal cancer cells. Drug Des. Devel. Ther. 1449–1460.

Li, B., et al., 2019. Isobavachalcone exerts anti-proliferative and pro-apoptotic effects on human liver cancer cells by targeting the ERKs/RSK2 signaling pathway. Oncol. Rep. 41 (6), 3355–3366.

Li, R., et al., 2022. Integrated multispectroscopic analysis and molecular docking analyses of the structure-affinity relationship and mechanism of the interaction of flavonoids with zein. Food Chem. 386, 132839.

Li, C.-Y., et al., 2022. Discovery and characterization of naturally occurring chalcones as potent inhibitors of bile salt hydrolases. Acta Mater. Med. 1 (2), 164–176.

Li, D., Hu, C., Li, H., 2018. Survivin as a novel target protein for reducing the proliferation of cancer cells. Biomed. Rep. 8 (5), 399–406.

Liang, M., et al., 2018. l-Arginine induces antioxidant response to prevent oxidative stress via stimulation of glutathione synthesis and activation of Nrf2 pathway. Food Chem. Toxicol. 115, 315–328.

Li-li, S., Wei-wei, W., Yun, S.U.N., 2014. Apoptosis of imatinib-sensitive and imatinib-resistant chronic myelocytic leukemia cells induced by isobavachalcone. J. Shanghai Jiaotong Univ. (Med. Sci.) 34 (9), 1309.

Luo, Y., Ma, J., Lu, W., 2020. The significance of mitochondrial dysfunction in cancer. Int. J. Mol. Sci. 21 (16), 5598.

Ma, L., et al., 2021. Plant natural products: Promising resources for cancer chemoprevention. Molecules 26 (4), 933.

Marini, H.R., et al., 2023. Glutathione: Lights and shadows in cancer patients. Biomedicines 11 (8), 2226.

Martínez-García, D., et al., 2019. Therapeutic strategies involving survivin inhibition in cancer. Med. Res. Rev. 39 (3), 887–909.

Miles, A.J., Janes, R.W., Wallace, B.A., 2021. Tools and methods for circular dichroism spectroscopy of proteins: A tutorial review. Chem. Soc. Rev. 50 (15), 8400–8413.

Ni, Y.-L., et al., 2019. Nerolidol suppresses the inflammatory response during lipopolysaccharide-induced acute lung injury via the modulation of antioxidant enzymes and the AMPK/Nrf-2/HO-1 pathway. Oxid. Med. Cell. Longev. 2019.

Niedernhofer, L.J., et al., 2003. Malondialdehyde, a product of lipid peroxidation, is mutagenic in human cells. J. Biol. Chem. 278 (33), 31426–31433.

Panada, J., et al., 2023. Differential induction of C6 glioma apoptosis and autophagy by 3β-hydroxysteroid-indolamine conjugates. Steroids, 109326.

Roslan, A.A., Tayyab, S., 2019. Exploring ligand–protein interaction: A laboratory exercise on herbicide binding to plasma transport protein. Biochem. Mol. Biol. Educ. 47 (2), 156–160.

Sabour, R., Harras, M.F., Mehany, A.B.M., 2020. Design, synthesis, cytotoxicity screening and molecular docking of new 3-cyanopyridines as survivin inhibitors and apoptosis inducers. Bioorg. Chem. 94, 103358.

Shi, Y., et al., 2017. Isobavachalcone inhibits the proliferation and invasion of tongue squamous cell carcinoma cells. Oncol. Lett. 14 (3), 2852–2858.

Shi, Y., et al., *Inhibitory effect of isobavachalcone on migration and invasion of Tca8113 cells and its mechanism.* Chinese Pharmacological Bulletin, 2015: p. 1741-1744, 1745.

Siddiqui, S., et al., 2021. Studying the interaction of drug/ligand with serum albumin. J. Mol. Liq. 336, 116200.

Simpson, J., Scholefield, J.H., 2008. Treatment of colorectal cancer: surgery, chemotherapy and radiotherapy. Surgery (Oxford) 26 (8), 329–333.

Singh, V.K., et al., 2019. Phytochemicals based chemopreventive and chemotherapeutic strategies and modern technologies to overcome limitations for better clinical applications. Phytother. Res. 33 (12), 3064–3089.

Sun, Y., et al., 2024. Comparative study on interactions of phillyrin and phillygenol with lysozyme: Spectroscopy, differential scanning calorimetry and molecular modeling approaches. J. Mol. Liq., 124571

Szliszka, E., et al., 2009. Chalcones enhance TRAIL-induced apoptosis in prostate cancer cells. Int. J. Mol. Sci. 11 (1), 1–13.

Szliszka, E., et al., 2012. Targeting death receptor TRAIL-R2 by chalcones for TRAIL-induced apoptosis in cancer cells. Int. J. Mol. Sci. 13 (11), 15343–15359.

Tang, L., et al., 2020. Interaction mechanism of flavonoids on bovine serum albumin: Insights from molecular property-binding affinity relationship. Spectrochim. Acta A Mol. Biomol. Spectrosc. 239, 118519.

Togashi, D.M., Ryder, A.G., 2008. A fluorescence analysis of ANS bound to bovine serum albumin: binding properties revisited by using energy transfer. J. Fluoresc. 18, 519–526.

Touloumis, Z., Lazaris, A., Griniatsos, J., 2020. The prognostic significance of Caspase-3 and survivin expression in colorectal cancer patients. Age (Median+ IR) 70, 61–76.

Verdecia, M.A., et al., 2000. Structure of the human anti-apoptotic protein survivin reveals a dimeric arrangement. Nat. Struct. Biol. 7 (7), 602–608.

Wang, M., et al., 2021. Pharmacological review of isobavachalcone, a naturally occurring chalcone. Pharmacol. Res. 165, 105483.

Wang, R., et al., 2023. Survival rate of colorectal cancer in China: A systematic review and meta-analysis. Front. Oncol. 13, 1033154.

Wei, R., et al., 2021. Tagitinin C induces ferroptosis through PERK-Nrf2-HO-1 signaling pathway in colorectal cancer cells. Int. J. Biol. Sci. 17 (11), 2703.

Wu, D., et al., 2018. Pharmacological inhibition of dihydroorotate dehydrogenase induces apoptosis and differentiation in acute myeloid leukemia cells. Haematologica 103 (9), 1472.

Wu, C.-Z., et al., 2022. Isobavachalcone Induces Multiple Cell Death in Human Triple-Negative Breast Cancer MDA-MB-231 Cells. Molecules 27 (20), 6787.

Wu, Y., et al., 2022. Isobavachalcone's alleviation of pyroptosis contributes to enhanced apoptosis in glioblastoma: Possible involvement of NLRP3. Mol. Neurobiol. 59 (11), 6934–6955.

Yang, L., et al., 2019. Isobavachalcone reveals novel characteristics of methuosis-like cell death in leukemia cells. Chem. Biol. Interact. 304, 131–138.

Yang, Y., Meng, W.-J., Wang, Z.-Q., 2023. Immunotherapy with immune checkpoint inhibitors for advanced colorectal cancer: A promising individualized treatment strategy. Front. Biosci.-Landmark 28 (4), 69.

Yi, B., Zhang, L., Zhou, H., 2024. Interaction mechanism of nordentatin with human α-1 acid glycoprotein and human colorectal cancer HCT-116 cells. Arab. J. Chem. 17 (1), 105432.

Zhang, Q., et al., 2019. DUB3 deubiquitinates and stabilizes NRF2 in chemotherapy resistance of colorectal cancer. Cell Death Differ. 26 (11), 2300–2313.

Zhang, Y., et al., 2022. Isobavachalcone induces cell death through multiple pathways in human breast cancer MCF-7 cells. Nan Fang yi ke da xue xue bao= J. Southern Med. Univ. 42 (6), 878–885.

Zhao, J., et al., 2022. Insights from multi-spectroscopic analysis and molecular modeling to understand the structure–affinity relationship and the interaction mechanism of flavonoids with gliadin. Food Funct. 13 (9), 5061–5074.

Zhao, L., et al., 2022. Isobavachalcone disrupts mitochondrial respiration and induces cytotoxicity through ROS accumulation and Akt suppression. Toxicon 216, 28–36.

Zhu, H., et al., 2016. Apigenin induced apoptosis in esophageal carcinoma cells by destruction membrane structures. Scanning 38 (4), 322–328.